TELKOMNIKA, Vol.17, No.1, February 2019, pp.489~496
ISSN: 1693-6930, accredited First Grade by Kemenristekdikti, Decree No: 21/E/KPT/2018
DOI: 10.12928/TELKOMNIKA.v17i1.11636

Determination of solid material permittivity using T-ring resonator for food industry

Rammah A. Alahnomi*[1], Z. Zakaria[2], Zulkalnain Mohd Yussof[3], Tole Sutikno[4], Amyrul Azuan Mohd Bahar[5], Ammar Alhegazi[6],
[1,2,3,5,6]Center for Telecommunication Research and Innovation (CeTRI),
Universiti Teknikal Malaysia Melaka (UTeM), Hang Tuah Jaya, Durian Tunggal, Melaka, Malaysia
[4]Department of Electrical Engineering, Universitas Ahmad Dahlan, Yogyakarta, Indonesia
*Corresponding author, e-mail: alrammah89@gmail.com[1], zahriladha@utem.edu.my[2]

Abstract

In this paper, we present a simple design of a T-ring resonator sensor for characterizing solid detection. The sensor is based on a planar microwave ring resonator and operating at 4.2 GHz frequency with a high-quality factor and sensitivity. An optimization of the T-ring geometry and materials were made to achieve high sensitivity for microwave material characterizations. This technique can determine the properties of solid materials from range of 2 GHz to 12 GHz frequencies. Techniques of current microwave resonator are usually measuring the properties of material at frequencies with a wide range; however, their accuracy is limited. Contrary to techniques that have a narrowband which is normally measuring the properties of materials to a high-accuracy with limitation to only a single frequency. This sensor has a capability of measuring the properties of materials at frequencies of wide range to a high-accuracy. A good agreement is achieved between the simulated results of the tested materials and the values of the manufacturer's Data sheets. An empirical equation has been developed accordingly for the simulated results of the tested materials. Various standard materials have been tested for validation and verification of the sensor sensitivity. The proposed concept enables the detection and characterization of materials and it has miniaturized the size with low cost, reusable, reliable, and ease of design fabrication with using a small size of tested sample. It is inspiring a broader of interest in developing microwave planar sensors and improving their applications in food industry, quality control and biomedical materials.

Keywords: *material characterization, microwave sensor, planar sensor, transmission line resonator*

1. Introduction

Recent developments in microwave resonator sensors, such as planar sensors, has motivated a growing research interest in high accuracy resonator designs. It is well-known that the microwave planar sensor is one of the most active areas in characterizing and detecting the dielectric material properties. This is due to its advantages of having simplicity in circuit designs and low-cost fabrication process. Numerous studies have been demonstrated various design approaches of microwave sensors for characterizing solid and liquid materials [1–13]. Concerning water content, studies have been done on the potential applications of microwave sensors in the food industry such as measuring the dielectric properties of several fresh fruits, hard red winter wheat, a fresh chicken breast and meat [14–15].

A common method is presented by Author in [16] and used to find the quality factor of half-wave line transmission resonators [17]. Generally, the half-wave resonator has been used for determining the attenuation of transmission line which can be easily measured at high frequencies. However, the half-wave line resonator has disadvantages of having large size of substrate area, and less accuracy measurement for higher frequencies causes by radiation losses of coupling gaps as indicated in Figure 1. Therefore, the quarter-half wave resonator is developed for reducing the radiation, improving the accuracy of measurement, and minimizing the circuit size.

In this paper, a quarter-wave T-ring resonator stub is developed in order to characterize the properties of solid materials. The T-ring resonator design is presented with all the mathematical and theoretical calculation used in analysis. The T-ring microstrip resonator method can be used for sensing application such as quality control of food industry and bio-sensing.

Received May 31, 2018; Revised October 16, 2018; Accepted November 19, 2018

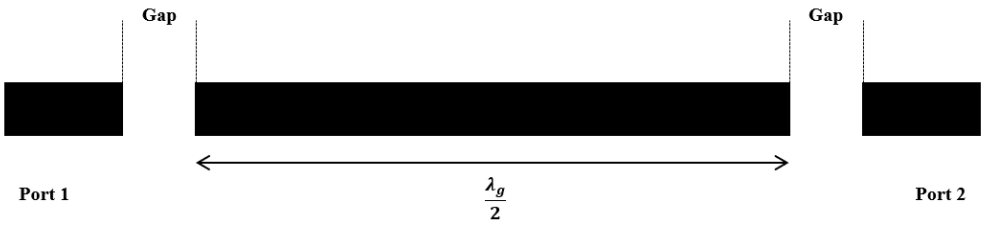

Figure 1. Half-wave line resonator structure for measuring attenuation

2. Research Method

Figure 2 demonstrates the configuration and design parameters of open T-stub resonator base on quarter-wave transmission. Roger RT/Duroid 5880 is used as substrate materials with thickness of 0.787 mm, loss tangent of 0.0009, permittivity of 2.2, and copper thickness of 17.5 µm. The proposed sensor has a dimension of cross section 37 mmx27 mm, (Wg, Lg) respectively, at operating frequency of 4.2 GHz. The width of the microstrip line can be found from [18].

The circuit of open stub quarter-wave line transmission creates a response of band stop (S21). The stub can be modelled and replaced by a circuit of lumped element resonator at near the resonance of stub as demonstrated in Figure 3. The two-port network (S21) in Figure 3 can be calculated at or near resonance using (1) [14]:

$$S_{21} = \frac{2Z_{in}}{2Z_{in} + Z_o} \quad (1)$$

where Z_o is the characteristic impedance of the measured system and Z_{in} is the input equivalent impedance for the resonator of the lumped element demonstrated in Figure 3.

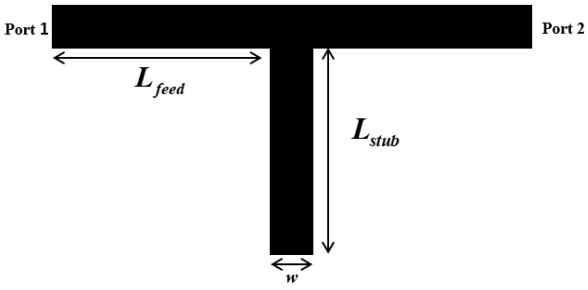

Figure 2. Configuration of open T-stub resonator based on quarter-wave transmission

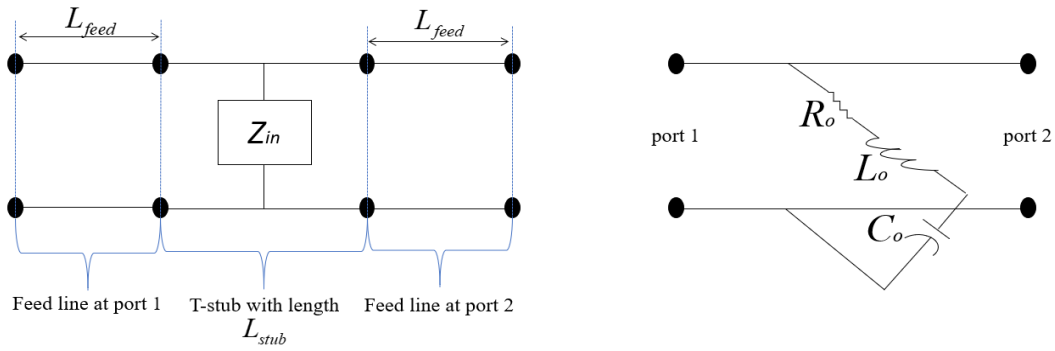

Figure 3. The circuit of the lumped element resonator at near resonance of stub

The microstrip line width can be formulated using (2) from [18]:

$$Z_o = \frac{120\pi}{\sqrt{\varepsilon_{eff}}\left[\frac{w}{d}+1.393+0.667\ln\left(\frac{w}{d}+1.444\right)\right]} \quad (2)$$

where:

$$\varepsilon_{eff} = \frac{\varepsilon_r+1}{2}+\frac{\varepsilon_r-1}{2}\frac{1}{\sqrt{1+\frac{12d}{w}}} \quad (3)$$

where ε_r is the substrate permittivity, W is the width of the microstrip conductor line, h is the thickness of substrate, ε_{eff} is the dielectric effective permittivity for medium of a homogenous that replaces the air region and the dielectric of the microstrip. The copper trace of the microstrip line width W is matched with an input and output 50 Ω SMA connectors and Vector Network Analyser.

The open-ended stub length is selected as a quarter wave-lengths at 4.2 GHz operating frequency. The stub length can be approximately modeled with the fundamental equation for a resonator of quarter-wave [19]:

$$L = \frac{nc}{4f\sqrt{\varepsilon_{eff}}} \quad (4)$$

where:

n is the resonance order (n=1,3,5,…)
c is the light speed
f is the resonance frequency
ε_{eff} is the dielectric effective constant.

the Q-factor of resonant frequency can be found by using the following equation:

$$Q = \frac{f_o}{B.W} \quad (5)$$

where:

Q is the measurement of quality-factor
f_o is the resonant frequency (MHz)
$B.W$ is the bandwidth at 3dB (MHz)

3. Results and Analysis

3.1. Location of Material under Test (MUT)

The change of the resonance frequency behavior is based on the interacting the electric field of the T-ring resonator with the test materials which is known as material under test (MUT). Therefore, it is mainly important to determine the region for locating the MUT for accuracy and sensitivity of the measurement where in this case; a maximum electric field of T-ring resonator is demonstrated in Figure 4 (a) (The red color illustrates the most electric field region). The MUT is overplayed on the copper track of the T-ring resonator substrate as shown in Figure 4 (b). The MUT perturbs the field distribution of T-ring resonator that causes a shifting in resonant frequency response and reduction in quality factor. The response of the resonant frequency variation is based on the MUT that has different permittivity and properties. Figure 4 (c) illustrates the perturbation theory between the MUT and electric field of T-ring resonator where the perturbation to the sensor can be determined by the location and the size of the tested material.

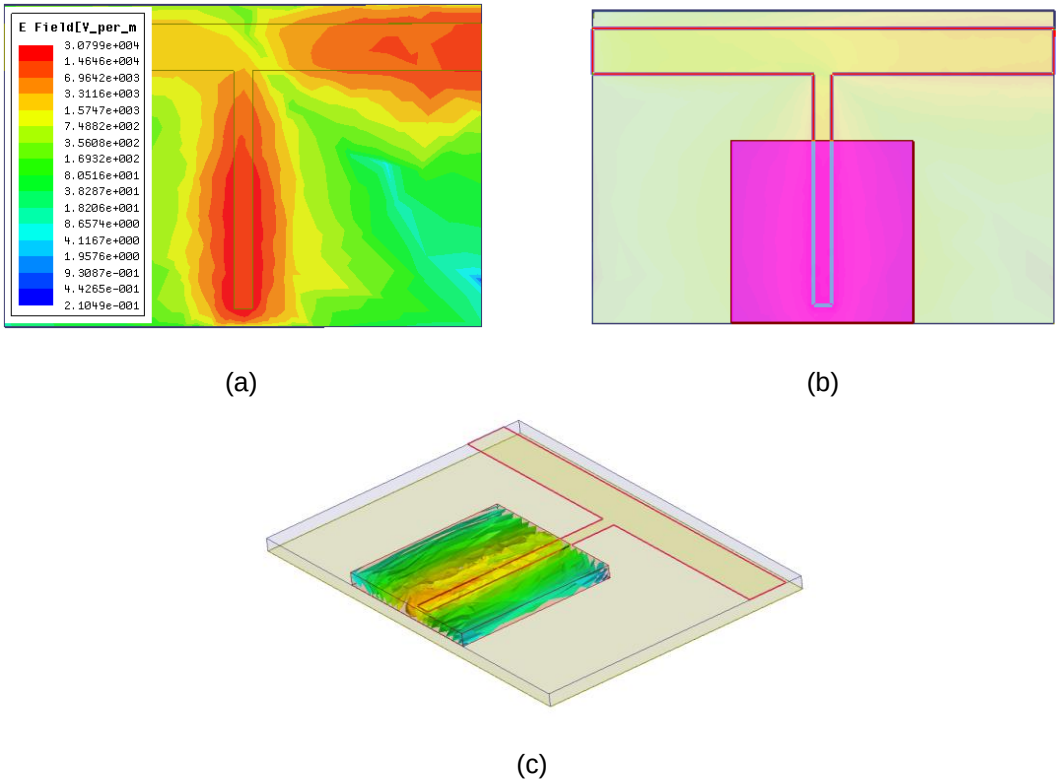

Figure 4. The possible location of tested materials for measurements
(a) maximum electric field location (red color shows the maximum), (b) overlay sample size,
(c) the MUT perturbs the electric field of T-ring resonator

3.2. Frequency Analysis

Simulation result of T-ring resonator without overlay soild smaple is illustrated in Figure 5. The obtained resonant frequency is occured at 4.2030 GHz operating frequency with a frequency range between 2 GHz to 12 GHz. It can clearly be seen that the T-ring resonator has a narrower stop-band and sharper dip that reveals its high quality factor. Furthermore, the results illustrate some small deviation between the theory calculated by (2) and the simulation. The simulated frequency is slightly shifted from the theory by 3 MHz to the higher frequency.

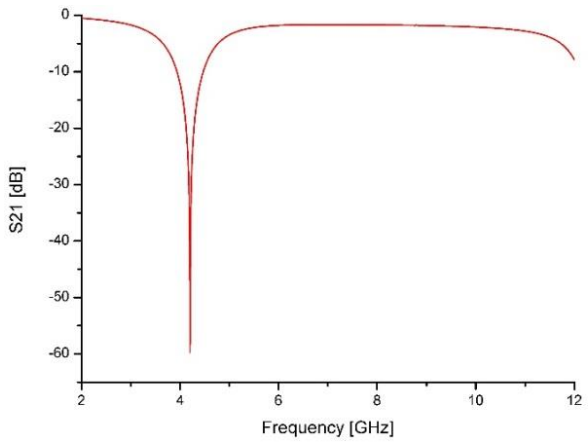

Figure 5. Simulated result of the transmission coefficients for T-ring resonator

3.3. Sensitivity Analysis

The response of the T-ring resonant frequency is dependent on the dielectric constant of the surrounding materials. Thus, when the tested material with different value of permittivity is tested on the T-ring, the electric field of the resonator is perturbed and causes a change in the resonant frequency. The tested materials are loaded where the maximum electric field of the T-ring resonator is generated as illustrated in Figure 6.

To quantify sensitivity, the unloaded T-ring resonator frequencies (Air) along with loaded materials (Roger 5880, Roger 4350, and FR-4) are simulated. It can be demonstrated that the relative change of the resonant frequency (Δf) and corresponding permittivity ($\Delta \varepsilon$) is linear. The T-ring sensor sensitivity S, is defined as (if T-ring sensor is loaded with FR-4 sample):

$$Sensitivity, S = \frac{\Delta f}{\Delta \varepsilon} = \left| \frac{f_{Air} - f_{FR4}}{\varepsilon_{Air} - \varepsilon_{FR4}} \right| \quad (6)$$

where: $\Delta \varepsilon$ is the change permittivity of tested material corresponding

Δf is the change of frequency

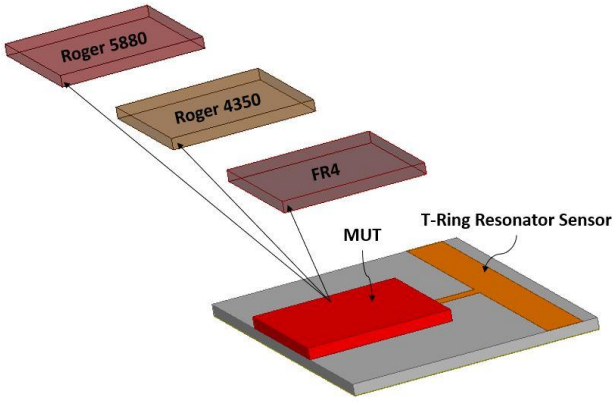

Figure 6. Testing the standard materials on the T-ring resonator sensor

To validate the results of T-ring resonator sensor, several solid materials with a standard permittivity have been tested. Figure 7 demonstrates the frequency responses of those standard materials. It is obvious that the response frequency is shifted to lower frequency and it is dependent on the tested material properties. FR4 material with a standard permittivity of 4.4 has the highest shift among others since it has the highest value of permittivity. The shifting percentage is about 3% compared to the unloaded T-ring resonator sensor.

Three MUT smaple materials have been tested with a permittivity ranging from 1 to 4.4. The coated copper layer of tested FR-4 were completely removed to realize a thickness of 1.6 mm with a permittivity of 4.4. Similary, Roger 5880 and Roger 4350 were used to realize a thickness of 0.789 mm and 0.508 mm with a permittivity value of 2.2 and 3.48, respecitvely [20]. Figure 7 demonstrates the change of transmission coefficient with respect to the change of sample permittivity of the tested material. As expected using analytical simulations, the resonant is shifted to lower frequency when increasing the MUT permittivity and a minimum transmission coefficient is obsereved. If we consider the result of high loss tangent such as FR-4 material with permittivity of 4.4, the shift is about 18%. While Roger 5880 has a shift of 10% since it has a low loss tangent with permittivity of 2.2.

Range of dielectric samples between 1 to 10 are tested and simulated in the T-ring resonator sensor for visualizing the sensing of the design applications. Figure 8 illustrates the resonant frequency shifting to lower frequencies accordingly when increasing the value of permittivity of the tested material. This is due to the interaction between the T-ring sensor

electric field and high capacitance particularly when placing the dielectric materials that absorbs the electric field of the sensor.

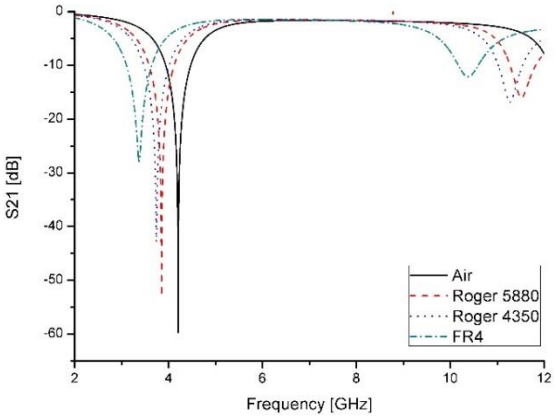

Figure 7. Change in transmission coefficients when changing material under test

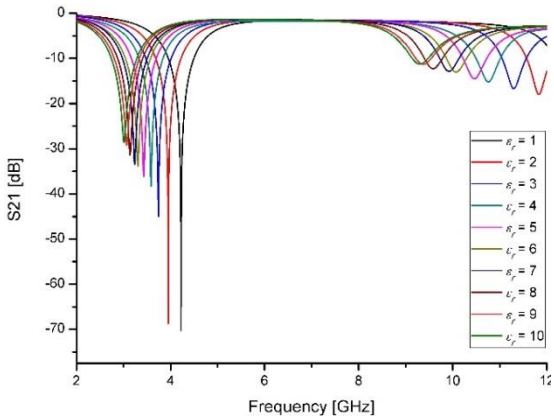

Figure 8. The change of T-ring resonant frequency with respect to MUT permittivity variation

To visualize the sensing application of the designed sensor, a MUT sample with varying the permittivity from 1 to 10 were loaded and simulated. The result is illustrated in Figure 9, where the resonant frequency is shifted down accordingly. This is because of the interaction between the electric field of the sensor and the loaded MUT where increasing the permittivity of MUT will cause a frequency shift. Furthermore, an empirical equation has been developed for the permittivity of MUT and the resonant frequency relationship. This empirical equation can be modeled based on curve fitting technique using 2nd order polynomial for the presented data in Figure 9 and it can be formulated as follows:

$$\varepsilon_r = 4.88f^2 - 42.36f + 92.99 \quad (7)$$

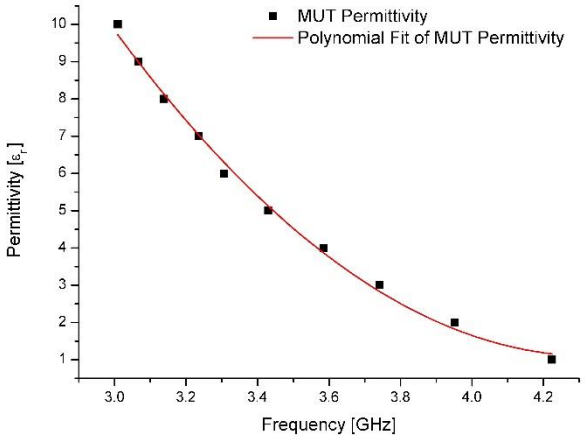

Figure 9. The 2nd order polynomial fit for various value of MUT permittivity with respect to resonance frequency

The sensitivity and resonant frequency is affected by the amount of sample's thickness for under loaded condition. Figure 10 illustrates the designed T-ring sensor for measuring the material of known and un-known permittivity. An investigation of the sample's thickness has been presented in Figure 11 where a 6 mm is considered as a lowest sample's thickness to test

materials. However, for more reliability and accuracy of the detection limits; an average thickness value of 10 mm is used as reporting limits for the T-ring sensor. It can be seen from the Figure 11 that the smaller sample thickness is affecting the resonant frequency since the thickness of sample is considered to be smaller than the penetration depth of electric field inside the sample and it remains constant for larger value of sample's thickness. Therefore, a further increment of sample's thickness will not affect the resonant frequency and sensitivity of the sensor.

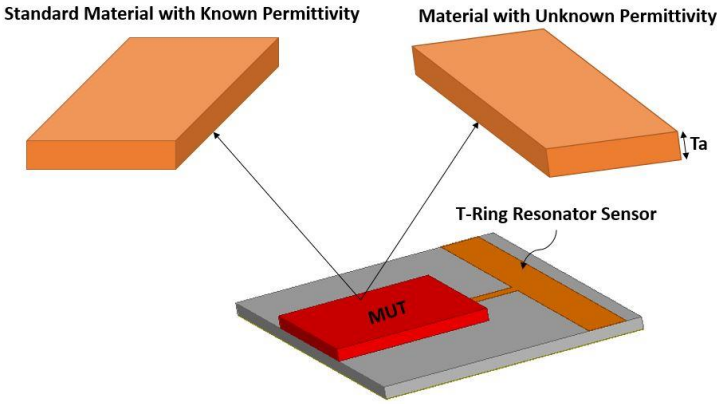

Figure 10. The designed T-ring sensor for testing material with known and unknown permittivity.

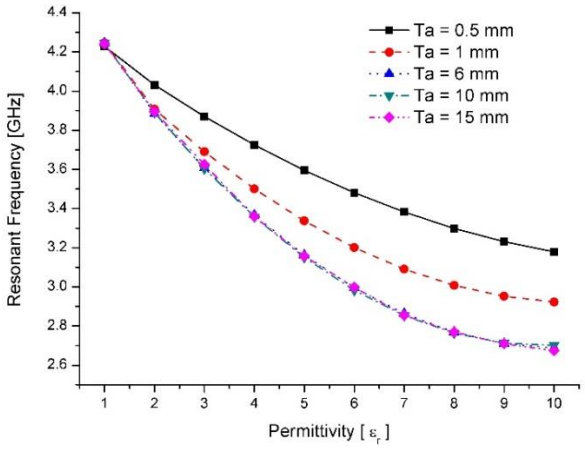

Figure 11. The change of various value of sample's thickness and real permittivity with respect to resonant frequency

4. Conclusion

This paper proposes a T-ring resonator solid material sensor. The solid sensor is composed of T-ring of quarter wave transform which is etched on the top of a substrate. A MUT is placed on the most sensitive area of the T-ring patch. When a solid is placed on the top of the T-sensor, the resonant frequency is changed due to the variation of effective permittivity. The proposed solid T-ring resonator is realized on substrate of Rogers Duroid 5880 at 4.2 GHz operating resonant frequency. The performance of the solid sensor is validated using three standard materials with known permittivity and the results illustrates a unique frequency response when the permittivity of known materials changed from 1 to 4.4 (Air with εr=1, Roger 5880 with εr=2.2, Roger 4350 εr=3.45, and FR4 εr=4.4). The T-ring resonator is miniaturized the size with low cost, reusable, reliable, and ease of design fabrication with using a small size of tested sample which makes it a suitable candidate for measuring low materials permittivity at

normal case under room temperature. For future consideration, we are planning to test various chemicals materials for evaluating the selectivity of the proposed solid sensor in medical applications.

Acknowledgments

This work was supported by UTeM Zamalah Scheme. The authors would also like to thank Centre for Research and Innovation Management (CRIM), Centre of Excellence, UTeM, UTeM's research grant PJP/2017/FKEKK/HI10/S01532 and Universiti Teknikal Malaysia Melaka (UTeM) for their encouragement and help in sponsoring this study.

References

[1] Vélez P, Su L, Grenier K, Dubuc D, Martín F. Microwave Microfluidic Sensor based on a Microstrip Splitter / Combiner Configuration and Split Ring Resonators (SRR) for Dielectric Characterization of Liquids. *IEEE Sensors Journal, Inst Electr Electron Eng*. 2017; 1748(c): 1–10.
[2] Muhammed Shafi KT, Ansari MAH, Jha AK, Akhtar MJ. Design of SRR-based microwave sensor for characterization of magnetodielectric substrates. *IEEE Microw Wirel Components Lett*. 2017; 27(5): 524–6.
[3] Porwal P, Syed A, Bhimalapuram P, Sau TK. Design of Rf Sensor for Simultaneous Detection of Complex Permeability and Permittivity of Unknown Sample. *Prog Electromagn Res C*. 2017; 79: 159–73.
[4] Mohd Bahar AA, Zakaria Z, Ab Rashid SR, Isa AAM, Alahnomi RA. High-efficiency microwave planar resonator sensor based on bridge split ring topology. *IEEE Microw Wirel Components Lett*. 2017; 27(6).
[5] Then YL, You KY, Dimon MN, Lee CY. *A modified microstrip ring resonator sensor with lumped element modeling for soil moisture and dielectric predictions measurement*. Meas J Int Meas Confed. 2016; 94: 119–25.
[6] Bakir M. Electromagnetic-Based Microfluidic Sensor Applications. *J Electrochem Soc*. 2017; 164(9): B488–94.
[7] Azuan A, Bahar M, Zakaria Z, Rosmaniza S, Rashid A, Isa AA. *Microstrip Planar Resonator Sensors for Accurate Dielectric Measurement of microfluidic solutions*. 3rd Int Conf Electron Des. 2016; 416–21.
[8] Amyrul Azuan MB, Zakaria Z, Rashid SRA, Isa AAM, Alahnomi RA. Dielectric Analysis of Liquid Solvents Using Microwave Resonator Sensor For High. *Microw Opt Technol Lett*. 2017; 59(2): 367–71.
[9] Alahnomi RA, Zakaria Z, Ruslan E, Bahar AAM. Microwave Sensors Based on Novel Symmetrical Split Ring Resonator. *Meas Sci Rev*. 2016; (1): 21–7.
[10] Alahnomi RA, Zakaria Z, Ruslan E, Mohd Bahar. AA, Ab Rashid SR. High sensitive microwave sensor based on symmetrical split ring resonator for material characterization. *Microw Opt Technol Lett*. 2016; 58(9): 2106–10.
[11] Alahnomi RA, Zakaria Z, Ruslan E, Ab Rashid SR, Mohd Bahar AA, Shaaban A. Microwave bio-sensor based on symmetrical split ring resonator with spurline filters for therapeutic goods detection. *PLoS One*. 2017; 12(9).
[12] Alahnomi RA, Zakaria Z, Ruslan E, Ab Rashid SR, Mohd Bahar AA. High-Q sensor based on symmetrical split ring resonator with spurlines for solids material detection. *IEEE Sens J*. 2017; 17(9).
[13] Abdolrazzaghi M, Zarifi MH, Pedrycz W, Daneshmand M. Robust Ultra-High Resolution Microwave Planar Sensor Using Fuzzy Neural Network Approach. *IEEE Sens J.* 2017; 17(2): 323–32.
[14] Nelson S. O., Trabelsi S . Dielectric Spectroscopy Measurements on Fruit, Meat, and Grain, Am. Soc. Agric. Biol. Eng., 2008; 51(5): 1829–1834.
[15] Clerjon S., Damez J . Microwave sensing for an objective evaluation of meat ageing. *J. Food Eng*. 2009; 94(3–4): 379–389.
[16] Li M. New Technique to Measure Transmission Line Attenuation. *IEEE Trans Microw Theory Tech*. 1995; 33(1): 219–22.
[17] Goldfarb ME, Platzker A. Losses in GaAs microstrip. *IEEE Trans Microw Theory Tech*. 1990; 38(12): 1957–63.
[18] Pozar DM. Microwave Engineering. Fourth Edi. John Wiley & Sons, Inc; 2012.
[19] Lätti KP, Kettunen M, Strom JP, Silventoinen P. A review of microstrip T-resonator method in determining the dielectric properties of printed circuit board materials. *IEEE Trans Instrum Meas*. 2007; 56(5): 1845–50.
[20] Alahnomi R, Binti N, Hamid A, Zakaria Z, Sutikno T, Azuan A. Microwave Planar Sensor for Permittivity Determination of Dielectric Materials. *Indonesian J Elec Eng & Comp Sci*. 2018; 11(1): 362–71.